Unsupervised Learning Facial Parameter Regressor for Action Unit Intensity Estimation via Differentiable Renderer

Xinhui Song¹, Tianyang Shi¹, Zunlei Feng², Mingli Song² Jackie Lin¹, Chuanjie Lin¹, Changjie Fan¹, Yi Yuan^{1*}

¹NetEase Fuxi AI Lab (* Corresponding author)

²Zhejiang University

{songxinhui,shitianyang,linjie3,linchuanjie,fanchangjie,yuanyi}@corp.netease.com,{zunleifeng,brooksong}@zju.edu.cn

ABSTRACT

Facial action unit (AU) intensity is an index to describe all visually discernible facial movements. Most existing methods learn intensity estimator with limited AU data, while they lack of generalization ability out of the dataset. In this paper, we present a framework to predict the facial parameters (including identity parameters and AU parameters) based on a bone-driven face model (BDFM) under different views. The proposed framework consists of a feature extractor, a generator, and a facial parameter regressor. The regressor can fit the physical meaning parameters of the BDFM from a single face image with the help of the generator, which maps the facial parameters to the game-face images as a differentiable renderer. Besides, identity loss, loopback loss, and adversarial loss can improve the regressive results. Quantitative evaluations are performed on two public databases BP4D and DISFA, which demonstrates that the proposed method can achieve comparable or better performance than the state-of-the-art methods. WhatâĂŹs more, the qualitative results also demonstrate the validity of our method in the wild.

CCS CONCEPTS

• Applied computing \rightarrow Computer games; • Computing methodologies \rightarrow Computer vision.

KEYWORDS

AU Intensity Estimation; Differentiable Renderer

ACM Reference Format:

Xinhui Song¹, Tianyang Shi¹, Zunlei Feng², Mingli Song² and Jackie Lin¹, Chuanjie Lin¹, Changjie Fan¹, Yi Yuan^{1*}. 2020. Unsupervised Learning Facial Parameter Regressor for Action Unit Intensity Estimation via Differentiable Renderer . In *28th ACM International Conference on Multimedia (MM '20), October 12–16, 2020, Seattle, WA, USA.*. ACM, New York, NY, USA, 10 pages. https://doi.org/10.1145/3394171.3413955

1 INTRODUCTION

Facial expression analysis is a research hotspot in computer vision and computer graphics. It can be useful in many applications, such

Permission to make digital or hard copies of all or part of this work for personal or classroom use is granted without fee provided that copies are not made or distributed for profit or commercial advantage and that copies bear this notice and the full citation on the first page. Copyrights for components of this work owned by others than the author(s) must be honored. Abstracting with credit is permitted. To copy otherwise, or republish, to post on servers or to redistribute to lists, requires prior specific permission and/or a fee. Request permissions from permissions@acm.org.

MM '20, October 12-16, 2020, Seattle, WA, USA.

© 2020 Copyright held by the owner/author(s). Publication rights licensed to ACM. ACM ISBN 978-1-4503-7988-5/20/10...\$15.00 https://doi.org/10.1145/3394171.3413955

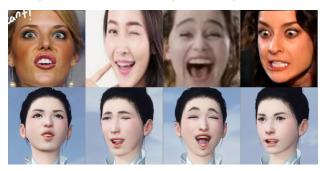


Figure 1: Visual results of our method. First row: face images with different expressions and different views; Second row: 3D characters generated with the predicted facial parameters, which are learned from the face images. Original photos in the first row are courtesy of Carrie Prejean, piotr marcinski, Emilia Clarke and Sin, respectively.

as human-robot interaction, social interaction analysis, and medical treatments. Facial expression analysis includes many research tasks: AU intensity estimation, 3D face reconstruction, facial expression recognition, facial action unit detection and so on. Among them, the AU intensity estimation [9] is the most challenging task, which aims to estimate anatomically meaningful parameters (i.e., muscle movements). Ekman and Friesen [9] develop a Facial Action Coding System (FACS) to characterize human expressions, which refers to a set of facial muscle movements that correspond to a displayed emotion. Nearly any anatomically possible facial expression can be coded by a combination of AUs. The difficulty of the AU intensity estimation steams from both the fine-grained analysis and meaningful parameters separated from different individuals. That is to say, the different individuals can dramatically increase variances of face images even when they have the same expression. Besides, pose also brings a challenge. Recently, some AU intensity estimation methods [21, 33, 47, 54-57, 60] require a large set of labeled training corpus, whether it is a fully supervised method or weakly supervised method. However, AU annotation requires strong domain expertise, resulting in very high time-and-labor costs to construct an extensive database.

3D face reconstruction is used to estimate a personalized human face model from a single photo. Recently, it is expanded to describe facial shapes and expressions. Many representative methods model the human face by estimating the coefficients of the 3D Morphable Models (3DMM) [3] or the 3D Based Face Model [30]. The 3D models are obtained from scan databases of limited size so that the

faces are constrained to lie in a low-dimensional subspace. Whereas, some algorithms do not generalize well beyond the restricted low-dimensional subspace of the 3DMM.

The bone-driven face model we adopted and used in the existing works [36, 39] is a character face rendering model of the game Justice¹. Meanwhile, similar face models are popularly used in many role-playing games (RPGs) (e.g., "Grand Theft Auto V", "Dark Souls III" and "A Dream of Jianghu"). The facial parameters of the BDFM are the facial component offsets to the base face and have explicit physical meanings. The "base face" is created by rendering a frontal emotionless face image, with the identity parameters set to 0.5. The identity parameters create a neutral face for an identity-specific face shape by controlling the attributes of facial components, including position, orientation, and scale. The offsets relative to the neutral face are baked to AU parameters, which can drive the facial muscle movement. The AU parameters can express almost all the AUs in FACS. They train a generator to make the bone-driven face model differentiable, and the facial reconstruction is formulated as an optimization problem. The iterative optimization process updates the facial parameters by minimizing the distance of the generated image and the input photo. However, the method has some limitations, including robustness and processing speed. Besides, the bone-driven face model has other additional challenges that some identity parameters corresponding images are meaningless and identity parameters tangle with AU parameters in some cases.

To solve the above problems, we present a trainable method to learn a facial parameter regressor \mathcal{G} with the help of a feature extractor F_{seg} , a generator and a face recognition network F_{reg} . We can train an end-to-end framework by using the rendered images to supervise the facial parameters fitting under the self-supervised paradigm. The inference speed is improved by two orders of magnitude than the optimization method. The overview of the proposed framework is shown in Fig. 2. The feature extractor F_{seg} extracts the shape-sensitive features. The facial parameter regressor is exploited to fit the facial parameters from the facial representation instead of the raw pixel image. The generator imitates the rendering process of game engines and makes the rendering process differentiable as introduced by previous methods [36, 39].

In the training phase, the network parameters of all networks are fixed except for the facial parameter regressor. The total loss function consists of five parts: facial content loss, identity loss, parameter loss, adversarial loss, and loopback loss. We utilize the facial content loss to measure the pixel-wise distance between the input face image and image generated with the predicted face parameters. The identity loss of the face recognition network F_{reg} can constrain the facial parameter regressor to match the identity features. The parameter loss and the adversarial loss are adopted to constrain the sparsity and disentanglement of the facial parameters, respectively. The loopback loss ensures the facial parameters regressor correctly interpret its output.

Our contributions are summarized as the following: 1) The first unsupervised method that estimates AU intensity from a single natural image without the AU annotations. 2) A pre-trained deep model that maps the facial parameters to a 3D character is incorporated into the framework to realize a differentiable framework.

3) Meanwhile, a disentangling mechanism is proposed to learn the mapping between the natural image and the facial parameters. 4) The proposed method achieves real-time prediction and SOTA performance.

2 RELATED WORKS

Learning to Regress 3D Face Models. Most methods [4, 7, 10, 18, 40, 42, 50] learn the coefficients of the 3D morphable model (3DMM) [3] to fit the input face image. Some previous approaches [4, 10] fit the 3DMM from a single face image by solving an optimization problem. However, these methods require expensive computation; moreover, they are sensitive to initialization. Deep learning methods [7, 18, 40, 42, 50] show the ability in regressing the 3DMM coefficients from a face image. However, these methods require an extensive collection of annotated training data, which is limited by 3D scan databases. One solution is to generate synthetic training data by sampling randomly from the 3DMM and rendering the corresponding faces [32]. Whereas, a deep network trained on purely synthetic data may present poorly due to the data is in limited condition. Other methods obtain the training data with an iterative optimization method, where the final optimized results are set as ground truth. However, the performance of those methods is always limited by the expressiveness of the iterative optimization method and the accuracy of the fitting process. For example, Tran et al. [42] propose a deep ResNet to regress the same 3DMM coefficients for different photos of the same subject. Due to the lack of training data, some unsupervised learning method are developed. For instance, Sanyal et al. [35] use RingNet to learn the 3D face shape. The RingNet leverages multiple images of a subject to train the model, which encourages the face shape to be similar when the identity is the same and different for different people. MOFA [41] contains a convolutional encoder network and an expert-designed generative model. The generative model is used to render the face with the 3DMM coefficients. Genova et al. [11] utilize the differentiable rasterizer to form neutral-expression face images. Inspired by the unsupervised learning methods, our approach can regress the meaningful facial parameters based on the differentiable rendering convolutional network without annotated data.

Supervised AU Intensity Estimation. Up to now, most of the works on automated AU analysis focus on AU detection. However, AU detection is a binary classification problem, so the methods can not estimate the AU intensity. AU intensity estimation is a more challenging task than AU detection and is a relatively new problem in the field. Recently, few works try to address it. Many [17, 19, 20, 28, 34] of these works independently estimate the AU intensity without considering the relationships among AUs. Considering the relationships, many researchers exploit the probabilistic graphical models [21, 33, 47]. Walecki et al. [47] use Copula Ordinal Regression (COR) to estimate the intensities of multiple AUs. Kaltwang et al. [21] exploit a latent tree model by conducting a graph-edits for representing the joint distribution of targets and features. Besides, temporal continuous is used in hidden Markov model [25] and continuous conditional neural fields (CCNF) [2]. Recently, several deep learning methods are proposed for AU intensity estimation, including CNN [12], CNN-IT [46] and 2DC [23]. These supervised learning methods require a large amount of annotated

 $^{^{1}}$ https://n.163.com/

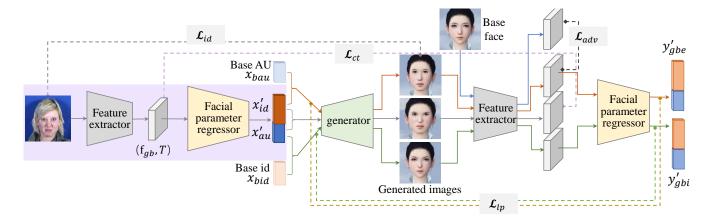


Figure 2: The learning framework for regressing meaningful facial parameters. The framework consists of four components: a feature extractor, a facial parameter regressor, a generator and a facial identity recognition network (not shown in the figure). The feature extractor is used to extract the facial features (f_{gb},T) . The facial parameter regressor is utilized to regress the facial parameters from the facial features. The generator is a differentiable renderer for mapping the facial parameters to the rendered image. In the training phase, only the network parameters of the facial parameter regressor are learnable, and they are updated by computing multiple losses with the generated images. The different colored lines mean the different flows. Only the part of the purple background is used in the predicting phase. Original image courtesy of MMI dataset.

images for training. However, annotating AU intensity is very difficult, which requires strong domain expertise. So it is expensive and laborious to construct an extensive database. With existing limited AU annotation data, supervise methods have two shortcomings: overfitting on the training set and limited AU expressions. However, our approach can estimate the AU intensity without AU annotated data and extend the number of estimable AU.

Weakly Supervised AU Intensity Estimation. A few weakly supervised methods [54-57, 60] use partially labeled images to train AU intensity estimation models. Zhao et al. [60] exploit the ordinal information to train a regressor with labeled and unlabeled frames among an expression sequence. Zhang et al. [54] propose a knowledge-based deep convolutional neural network for AU intensity estimation with peak and valley frames in training sequences. BORMIR [57] formulates the AU intensity estimation as a multiinstance regression problem with weakly labeled sequences. Zhang et al. [55] present a patch-based deep model consisting of a feature fusion module and a label fusion module. Zhang et al. [56] joint learn representation and intensity estimator to achieve an optimal solution with multiple types of human knowledge. However, these methods still require high-quality annotated training corpus. And the human-defined knowledge restricts the space of anatomically plausible AUs. Differently, our method requires neither a large scale of data nor restricts the space of AUs. It can still accurately regress multiple AUs with the help of the differentiable renderer.

2.1 Method

We expand an encoder-decoder architecture that permits learning of the meaningful facial parameters (Fig. 2). The training framework consists of four sub-networks: a feature extractor F_{seg} , a facial parameters regressive network \mathcal{R} , a facial generative network \mathcal{G} , and a face recognition network F_{reg} . The deep features extracted by the

feature extractor are the input of the facial parameters regressive network, which regresses the facial parameters. The facial generative network is a differentiable renderer, which renders expressive face images with the facial parameters under varying pose. The rendered face image is the input of the face recognition network and the feature extractor, which supervises the training of the facial parameters regressor. Only the facial parameter regressor's parameters are updated in the training phase, while the pre-trained feature extractor is fixed.

2.2 Generator

In the role-playing games, the parameterized physical model (the bone-driven face 3D model) is usually adopted to render a 3D character image. Each parameter of the parameterized model can control the facial component offset. However, the parameterized physical model is not differentiable. To make the whole framework differentiable, we train a generator to imitate the render process with the paired facial parameters and the rendered images. The generator $\mathcal{G}:y_g\longrightarrow I_{y_g}$ maps a set of meaningful facial parameters to a rendered image. The facial parameter y_g is a 269-dimensional vector with the head pose $h \in \mathbb{R}^{1 \times 2}$, AU parameters $y_{au} \in \mathbb{R}^{1 \times 23}$, and identity parameters $y_{id} \in \mathbb{R}^{1 \times 244}$. The identity parameter y_{id} contains the continuous 208-dimensional parameters and a discrete parameter, which represents 36 styles of the brown. The rendered image is generated with the bone-driven face 3D model. In other words, it is the ground truth $I_{y_g} \in \mathbb{R}^{H \times W \times 3}$. While, the generated image I'_{y_g} is generated with a deep model (generator). Our generations of the second of tor $\mathcal{G}(y_q)$ consists of eight transposed convolution layers, which is similar to the generator of DCGAN [31]. We use instance normalization [43] instead of batch normalization [16] for improving training stability in the generator, which is also used in GENet [39]. We aim to minimize the difference between the rendered image and

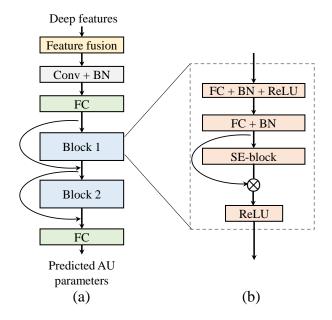


Figure 3: (a) The AU parameter regressive network. The regressive network consists of a feature fusion block, a convolution layer, two attention blocks and two fully connected (FC) layers. (b) The details of the attention block. \bigotimes means element-wise product. SE-block is similar to the squeeze and excitation block in SENet [15] and it is applied to an FC layer.

the generated one in the raw pixel space. We adopt a content loss (L_{app}) and a perceptual loss (L_{per}) between the rendered image I_{y_a} and the predicted one $I'_{y_a} = \mathcal{G}(y_g)$. The losses are defined as:

$$\mathcal{L}_{app}(y_g) = E_{y_g \sim u(y_g)}[\|I_{y_g} - I'_{y_g}\|_1], \tag{1}$$

$$\mathcal{L}_{per}(y_g) = E_{y_q \sim u(y_q)}[\|\mathcal{F}(I'_{y_q}) - \mathcal{F}(I_{y_g})\|_2]. \tag{2}$$

The two losses are combined to learn the generator ${\cal G}$ as:

$$\mathcal{L}_{\mathcal{G}}(y_g) = \mathcal{L}_{app}(y_g) + \lambda \mathcal{L}_{per}(y_g), \tag{3}$$

where y_g is the facial parameters sampled from a uniform distribution $u(y_g)$. $\mathcal F$ denotes the relu2_2, relu3_3, relu4_3 feature maps in VGG16 [38], which is pre-trained on the image recognition task. The λ is the balance parameter.

2.3 Feature Extractor

It's noticed that there is a large domain gap between the generated image and the real input image. To effectively measure the distance of the two images, we adopt a facial segmentation network as the feature extractor F_{seg} for extracting the face features, which has been proved effective in GENet [39]. Specifically, The feature extractor F_{seg} is based on the pretrained BiSeNet [51]² in our framework. I is the input face image or the generated one, which is aligned via five facial landmarks using affine transformation, including left eye, right eye, nose, left mouth corner, and right mouth corner.

The facial landmarks are obtained by OpenFace [1]. The feature f_{gb} extracted from the feature fusion module is used to describe the global information. And the latter three layers feature maps of ResNet18 [14] are extracted to describe the local information in the context path of BiSeNet. The feature extractor is defined as:

$$f_{qb}, T = F_{seq}(I), \tag{4}$$

where *T* is the set of the feature maps with weights.

Furthermore, an attention mechanism is deployed in the feature maps of the last three layers. It allows the feature maps to focus on different regions of the face. The output probability maps of the facial segmentation network serve as the attention masks, which are represented as the pixel-wise weights A in Eqn. (5). For example, the first layer's feature map is sensitive to the browns, and the element-wise sum of the browns' probability maps is multiplied to the feature map of the first layer. Suppose C is the set of the feature maps. The facial representation T is the set of multiple layers' output features, and one of them can be defined as:

$$\mathcal{T}_i = \beta_i A_i(I) C_i(I), \tag{5}$$

where β represents the weight of each feature map C_i . Specifically, the facial representation T consists of five components, including eyes \mathcal{T}_e , nose \mathcal{T}_n , mouth \mathcal{T}_m , face \mathcal{T}_f and brown \mathcal{T}_b . The features of eyes and browns are extracted from the first layer. The features of the second layer are sensitive to the nose and mouth. The facial silhouette is extracted from the feature of the third layer.

2.4 Facial Parameter Regressor

The straightforward idea is that regressing all the facial parameters together through a fully connected layer. However, each group of parameters has a strong meaning and responds to different features. The discovery has also been observed in multi-task learning work [59]. Intuitively speaking, the head pose is not sensitive to local features since it is fundamentally independent of facial identity and subtle facial expressions. Whereas, for identity, both local and global features are necessary to distinguish the different persons. The local and global features describe the shape of the four sense organs (including browns, eyes, nose, and mouth) and the overall facial silhouette, respectively. Similarly, expression describing requires fine-grained features, such as mouth raised, pout and eye closed. Therefore, we regress the facial parameters by different deep features, which are extracted from the feature extractor (BiSeNet). The feature f_{qb} is used to regress the head pose. The facial representation $(\mathcal{T}_e, \mathcal{T}_n, \mathcal{T}_m, \mathcal{T}_f)$ is utilized to fit the continuous identity parameters and AU parameters. The \mathcal{T}_b is used to regress the discrete identity parameters. The predicted facial parameters y' is defined as follows:

$$y' = \mathcal{R}(f_{qb}, T) = \mathcal{R}(F_{seq}(I)), \tag{6}$$

where I is the input face photo.

Specifically, the facial parameters regressor is separated into four sub-regressive networks: the head pose regressive network, the continuous identity parameters regressive network, the discrete identity parameters regressive network and the AU parameters regressive network. The four networks have similar network architecture, which is shown in Fig. 3. A sub-regressive network contains a feature fusion block, a convolution layer, two attention blocks, and

 $^{^2} https://github.com/zllrunning/face-parsing.PyTorch\\$

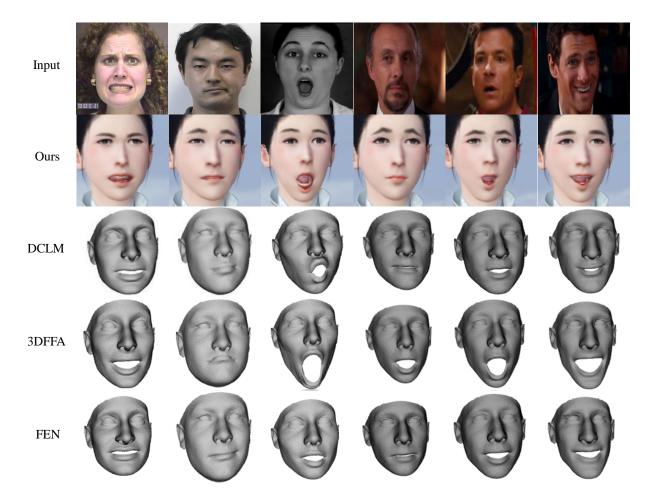


Figure 4: Qualitative comparison with other methods. The results are shown in the same viewpoint. The results of DCLM [52], 3DFFA [61] and FEN [6] are from original paper. The first three images are courtesy of FEN [6] in the first row. The last three original images are courtesy of Hector Elizondo, Jason Bateman, and Justin Bartha.

two fully connected (FC) layers. We first append a global average pooling layer for different feature maps to resize the feature maps to the same size. And then concatenate the output features, called "feature fusion". A convolution layer is performed with stride=2, followed by batch normalization. The detail of the attention block is shown in Fig. 3 (b). Similar to the squeeze and excitation block in SENet [15], we apply it to an FC layer, called "SE-block".

2.5 Losses

We propose a novel loss function that jointly regresses the head pose, identity parameters, and AU parameters. The loss function is conceptually straightforward and enables unsupervised training of our network. It combines five terms:

$$\mathcal{L} = \mathcal{L}_{ct} + w_{id}\mathcal{L}_{id} + w_{pr}\mathcal{L}_{pr} + w_{lp}L_{lp} + w_{adv}\mathcal{L}_{adv}, \quad (7)$$

where, L_{ct} measures the pixel-wise distance of the facial representation from a pre-trained facial feature extractor, \mathcal{L}_{id} preserves the identity information on the real images, \mathcal{L}_{pr} is utilized to learn the sparse facial parameters, \mathcal{L}_{lp} ensures the network can correctly

interpret the generated one, and \mathcal{L}_{adv} regularizes the predicted identity parameters.

Facial Content Loss. To constrain the facial shape's similarity between the "generated" result and the real input image, we define a facial content loss by computing the pixel-wise distance based on the facial representation T, which is introduced in Sec. 2.3. The facial content loss \mathcal{L}_{ct} is defined as:

$$\mathcal{L}_{ct} = \|T_g - T_r\|_1,\tag{8}$$

where T_g and T_r denote the facial representations of the generated and the real facial image, respectively.

Identity Loss. To effectively disentangle the identity and AU parameters, we add the identity loss to measure the similarity between the input image and the emotionless generated one. The facial recognition network F_{reg} named LightCNN-29v2 [49]³ is adopted to extract 256-d face embedding as the identity representation. The cosine similarity [48] of two images is set as the identity

 $^{^3} https://github.com/AlfredXiangWu/LightCNN\\$

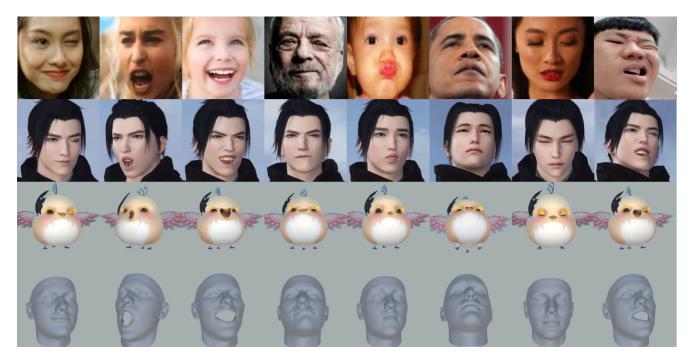


Figure 5: Retargeting from faces to other 3D characters. The first row is the input images and the last three rows represent the results of transferring the head pose and AU parameters to other 3D characters. Original images courtesy of Yin Zhu, Emilia Clarke, pobhble 3ykn, Stephen Joshua Sondheim, Jackson, Barack Obam, HHFQ [22], and Jackie Lin (ours), respectively.

loss, which is defined as:

$$\mathcal{L}_{id} = 1 - \cos(m_{qbe}, m_r) = 1 - \cos(F_{reg}(I_{y_{qbe}}), F_{reg}(I)),$$
 (9)

where m_{gbe} and m_r are the identity embeddings of the emotionless generated image $I_{y_{gbe}}$ (is known as the generated image with "base AU") and the real input image I from the facial recognition network, respectively. The "base AU" represents all the AU parameters setting to 0.02.

Parameter Loss. To the best of our knowledge, there exists the mutual exclusion of AUs in various facial expressions. For example, jaw left and jaw right, smile and lip stretcher can not occur at the same time. The same rule is applied to identity parameters. For an input image, we hope the predicted parameters are as sparsely as possible. The reason is that the dense parameters and the sparse parameters could have the same facial expression. For example, jaw left 0.5 can be generated by (turning right: 0.4, turning left: 0.9). Meanwhile, it can also be generated by (turning right: 0, turning left: 0.5). So, some parameters can counteract the inverse facial parameters. The parameter loss \mathcal{L}_{pr} is adopted to enforce a sparsity constraint, which is defined as follows:

$$\mathcal{L}_{pr} = \|h' - h_b\|_2^2 + \alpha \|x'_{id} - x_{bid}\|_2^2 + \beta \|x'_{au} - x_{bau}\|_2^2, \quad (10)$$

where, h', x'_{id} and x'_{au} denote the predicted head pose, identity and AU parameters, respectively. h_b, x_{bid} and x_{bau} denote the frontal head pose, base identity parameters and emotionless AU parameters, which are set to 0.5, 0.5 and 0.02, respectively. α and β are the balance parameters.

Loopback Loss. The true facial parameters of the real face images are unknown for unsupervised training. However, for the generated images, the true facial parameters are known. Inspired by the unsupervised 3D face reconstruction method proposed by Genova $et\ al.$ [11], we introduce the "loopback" loss, which constrains the consistency between the GT parameters and the predicted parameters of the image generated with the GT parameters. In the training stage, the extracted representations of the generated images I_{gbe} and I_{gbi} are fed into the facial parameter regressor to get the parameters y'_{gbe} and y'_{gbi} . I_{gbe} and I_{gbi} denote the generated images replaced by base AU and base identity. y_{gbe} and y_{gbi} are the facial parameter ground truths with base AU or base identity. So, $y_{gbe} = (x_{bau}, x'_{id})$ and $y_{gbi} = (x'_{au}, x_{bid})$. The loopback loss is defined as follows:

$$\begin{split} \mathcal{L}_{lp} &= \|y_{gbe} - y_{gbe}'\|_{1} + \lambda_{le} \|y_{gbi} - y_{gbi}'\|_{1} \\ &= \|y_{gbe} - \mathcal{R}(F_{seg}(I_{gbe})\|_{1} + \lambda_{le} \|y_{gbi} - \mathcal{R}(F_{seg}(I_{gbi})\|_{1}, \end{split}$$

where λ_{le} is the balance parameter.

Adversarial Loss. The bone-driven face model's identity parameters describe a large-scale 3D space where some points don't exist in the real world. To solve the problem, we adopt the adversarial loss to encourage the generated image indistinguishable from the "base face" in the mouth region. It makes the AU parameters to response for the facial muscle movement. And the identity parameters keep the facial outline and the position of the four sense organs. The "base face" I_b is created by rendering a frontal emotionless face image with the identity parameters setting to 0.5. The facial representation of the "base face" is represented to \mathcal{T}_{bm} in the mouth

Table 1: The Intra-Class Correlation (ICC) and Mean Absolute Error (MAE) on BP4D and DISFA. Bold numbers indicate the best performance. Underline numbers indicate the second best. (*) indicates results taken from the reference. ↑ means the higher, the better. ↓ means the lower, the better.

	Database	atabase BP4D						DISFA												
	AU	06	10	12	14	17	Avg	01	02	04	05	06	09	12	15	17	20	25	26	Avg
	KBSS [54]*	.76	.73	.84	.45	.45	.65	.23	.11	.48	.25	.50	.25	.71	.22	.25	.06	.83	.41	.36
	KJRE [56]*	.71	.61	.87	.39	.42	.60	.27	.35	.25	.33	.51	.31	.67	.14	.17	.20	.74	.25	.35
ICC	LBA [13]*	.71	.64	.81	.23	.50	.58	.04	.06	.39	.01	.41	.12	.73	.13	.27	.10	.82	.43	.29
icc	2DC [23]*	<u>.76</u>	.71	.85	.45	.53	<u>.66</u>	.70	.55	.69	.05	.59	.57	.88	.32	.10	.08	.90	.50	.50
1	CFLF [55]*	.77	.70	.83	.41	.60	<u>.66</u>	.26	.19	.46	.35	.52	.36	.71	.18	.34	.21	.81	.51	.41
	GENet [39]*	.69	.85	.73	.63	<u>.53</u>	.68	.66	<u>.67</u>	.73	.71	.60	.59	.60	.66	.58	<u>.45</u>	.80	.70	.64
	Ours	.67	.62	.67	.62	<u>.53</u>	.62	.64	.74	.59	<u>.67</u>	.63	<u>.58</u>	.55	<u>.61</u>	<u>.49</u>	.50	.71	<u>.66</u>	<u>.61</u>
	KBSS [54] *	.74	.77	.69	.99	.90	.82	.48	.49	.57	.08	.26	.22	.33	.15	.44	.22	.43	.36	.34
	KJRE [56]*	.82	.95	.64	1.08	.85	.87	1.0	.92	1.9	.70	.79	.87	.77	.60	.80	.72	.96	.94	.91
MAE	LBA [13]*	.64	.80	.56	1.10	.62	.74	.43	.29	.51	.10	.30	.19	.30	.11	<u>.31</u>	.14	.40	.38	.29
	2DC [23]*	.87	.84	.92	.67	.73	.81	.57	.62	.73	.51	.66	.55	.50	.52	.78	.42	.61	.74	.61
\downarrow	CFLF [55]*	.62	.83	.62	1.00	.63	.74	.33	.28	.61	.13	.35	.28	.43	.18	.29	.16	.53	.40	.33
	GENet [39]*	.45	.60	.37	.40	.27	<u>.42</u>	.36	.33	.38	.14	.34	.36	.57	.18	.42	.26	.27	.32	.33
	Ours	.44	.31	<u>.45</u>	<u>.48</u>	<u>.36</u>	.41	.40	<u>.21</u>	<u>.39</u>	.16	.28	.30	.51	<u>.15</u>	.32	.19	<u>.25</u>	.26	.29

region. I_{gbe} is the emotionless generated image. \mathcal{T}_{gbem} represents the facial representation of the input images I_{gbe} in the mouth region. It is one group of the facial representation T extracted from the feature extractor F_{seg} in the mouth region. The adversarial loss is defined as:

$$\mathcal{L}_{adv} = \|\mathcal{T}_{gbem} - \mathcal{T}_{bm}\|_1 = \|F_{seg}(I_{gbe}) - F_{seg}(I_b)\|_1. \tag{12}$$

3 EXPERIMENTS

3.1 Datasets

We combine multiple datasets as a training set to accurately predict the facial parameters. Facewarehouse [5] and MMI [29, 44] are rich datasets for expressions. DISFA [26, 27] and the Binghamton 4D (BP4D) [45, 53, 58] are the two largest expression databases for AU intensity estimation. Among them, DISFA contains 27 subjects, and the AU intensity of 12 AUs (1, 2, 4, 5, 6, 9, 12, 15, 17, 20, 25, 26) are annotated. We use 18 subjects for training and 9 subjects for testing. BP4D contains 41 subjects, and 5 AU intensity (6, 10, 12, 14, 17) are annotated. We use 21 subjects for training and 20 subjects for testing. The extended cohn-kanade dataset (CK+) [24] contains 123 objects. 100 objects are used for training. Due to the datasets are all frontal face images, so we augment them to multiple poses with the same identity and expression by the high-fidelity pose and expression normalization (HPEN) [62]. Besides, the expression distribution is nonuniform in the datasets. So we augment the data through warping the images according to 68 key points.

3.2 Training Set

We first train the facial generator with 80,000 paired samples, which are constituted of the facial parameters and the corresponding rendered images. And then we fixed the network parameters of the proposed framework except for the facial parameter regressor. We set $w_{id}=0.1, w_{pr}=0.1, w_{lp}=0.1$ and $w_{adv}=0.1$ in our framework. α and β are set to 0.1 and 0.01. λ_{le} is set to 1.

3.3 Compared with Other Methods

Qualitative results. We compare our method with several 3D face reconstruction methods, including DCLM [52], 3DFFA [61] and FEN [6]. Fig. 4 provides rendered results with the same head pose for CK+ and EmotiW-17 [8]. The second row shows the rendered results of the facial parameters estimated by our method. The other three methods are based on 3DMM and their results are from the paper [6]. These rendered images support that our qualitative results have better appearance than other methods. To evaluate our method's efficiency, we also show more estimation results and retarget facial motion to other 3D characters in Fig. 5. The input images are from the EmotionNet dataset and MS-SFN [7]. The 3D characters have the same meaningful AU parameters with the bone-driven face model. The results demonstrate that this approach can effectively disentangle facial parameters.

Quantitative results. In this section, the DISFA and BP4D are adopted to quantitatively evaluate the effectiveness of our method. Intra-Class Correlation (ICC(3,1) [37]) and Mean Absolute Error (MAE) are calculated to evaluate the AU intensity estimation methods between the ground truth and the predicted one. We compare our method with several popular supervised learning methods, including ResNet18 [14], CCNN-IT [46] and CNN [12]. CNN [12] is composed of three convolutional layers and a fully connected layer. CCNN-IT [46] takes advantage of CNNs and data augmentation. ResNet18 is introduced in [14]. These supervised methods require annotated AU intensity of each frame in sequences while ours does not need the AU annotations. Our method achieves better performance on both metrics (Table 2).

We also compare the proposed method with several state-of-the-art weakly-supervised learning methods (KBSS [54], KJRE [56] and CFLF [55]), a semi-supervised learning method (LBA [13]), a supervised method (2DC [23]) and an unsupervised method (GENet [39]). LBA [13] estimates unlabeled samples with the assumption that samples with similar labels have similar latent features. CFLF

Input



Full framework



No content



With landmark







Figure 6: Ablation test showing the appearance by removing facial content loss ("no content") or using landmark loss ("with landmark") to replace. Column 1 corresponds to the input and column 2 corresponds to the results of our method, which is called "full framework". The facial content loss is very important for keeping the results in the space of human faces. The facial landmark network can not capture the details of the facial appearance. Original images are courtesy of Barack Obama and Antonio Villaraigosa.

[55] uses the context-aware feature and label to train a patch-based deep model. 2DC [13] uses a semi-parametric VAE framework, while KBSS [54] and KJRE [56] exploit domain knowledge to train a deep model. Note that KBSS, KJRE, CFLF, LBA and 2DC need labeled data to train their models. GENet [39] updates the facial parameters by iterative optimization process. It takes 2 seconds to predict one image. Unlike them, we propose a framework for estimating AU intensity without annotated AU data. And this proposed method can improve two orders of magnitude than GENet. The quantitative results are listed in Table 1.

On the BP4D and the DISFA datasets, our method can achieve superior average performance over other methods with MAE. On DISFA, our method achieves the second-best with ICC. Note that ICC and MAE should be jointly considered to evaluate one method. LBA tends to predict the intensity to be 0, which is the majority of AU intensity. It can achieve good MAE performance, but its ICC is much worse than ours. During the training phase, KBSS and CFLF need multiple frames as input; hence it requires more than one image per face, which is not always available. These results show the superior performance of the proposed method over existing weakly and semi-supervised learning methods. Besides, we also notice that our method has a bad performance than GENet on ICC. But our method can improve two orders of magnitude speed.

3.4 Ablation Studies

We perform several ablation experiments to verify the effectiveness of four loss functions in our framework. The facial content loss Eqn. (8) is the critical loss function in our method. If no facial content loss, the facial parameter regressor can only learn the

Table 2: Comparison with several supervised methods on DISFA. (*) indicates results taken from the reference.

Method	CNN [12]*	ResNet18 [14]*	CNN-IT [46]*	Ours
ICC	.33	.27	.38	.61
MAE	.42	.48	.66	.29

Table 3: Ablations analysis on different loss functions of the proposed method.

	Loss f	unction	n	BI	P4D	DISFA ICC MAE		
\mathcal{L}_{id}	\mathcal{L}_{lp}	\mathcal{L}_{pr}	\mathcal{L}_{adv}	ICC	MAE	ICC	MAE	
×	✓	✓	✓ ✓ ✓ ×	.53	.65	.55	.35	
\checkmark	×	\checkmark	\checkmark	.60	.64	.52	.37	
\checkmark	\checkmark	×	\checkmark	.60	.62	.55	.33	
\checkmark	\checkmark	\checkmark	×	.58	.63	.55	.34	

identity parameters, not head pose or AU parameters. Beyond that, the facial landmark network is a popular basic task for describing facial features. We also use the facial landmark network instead of the feature extractor. Specifically, The last output heatmap and the features of the first two layers of the facial landmark network⁴ are used to describe the global and local information, respectively. And the facial content loss is replaced by MSE loss of the heatmaps. Experimental results demonstrate that the facial landmark network can not capture the detail information. Due to the significant differences between the results, so we only show server examples in Fig. 6. Besides, with the help of the identity loss Eqn. (9), our method can noticeably improve the results of the facial parameter regressor. For parameter loss Eqn. (10), adversarial loss Eqn. (12) and loopback loss Eqn. (11), we utilize the same evaluation metric as the quantitative comparison experiment. The quantitative ablation results are shown in Table 3. They can help our method to have a significant improvement.

4 CONCLUSION

This paper proposes an unsupervised learning framework for AU intensity estimation from a single face photo. Different from the previous weakly-supervised methods and iterative optimization method, our method can estimate AU intensity without any annotated data. And the facial parameters regressor can improve 100x computational speedup than the iterative optimization method. Quantitative and qualitative results have proved that the proposed method can achieve comparable results than other methods. The ablation analysis also explains the effectiveness of our method on the five components.

ACKNOWLEDGMENTS

This work is supported by National Natural Science Foundation of China (61976186), Key Research and Development Program of Zhejiang Province (2018C01004), and the Major Scientific Research Project of Zhejiang Lab (No. 2019KD0AC01).

 $^{^4} https://github.com/1 adrianb/face-alignment \\$

REFERENCES

- Tadas Baltrušaitis, Marwa Mahmoud, and Peter Robinson. 2015. Cross-dataset learning and person-specific normalisation for automatic action unit detection. In Automatic Face and Gesture Recognition, Vol. 6. IEEE, 1–6.
- [2] Tadas Baltrušaitis, Peter Robinson, and Louis-Philippe Morency. 2014. Continuous conditional neural fields for structured regression. In European Conference on Computer Vision. Springer, 593–608.
- [3] Volker Blanz and Thomas Vetter. 1999. A morphable model for the synthesis of 3D faces. In Computer Graphics and Interactive Techniques. 187–194.
- [4] Chen Cao, Qiming Hou, and Kun Zhou. 2014. Displaced dynamic expression regression for real-time facial tracking and animation. *Transactions on graphics* 33, 4 (2014), 1–10.
- [5] Chen Cao, Yanlin Weng, Shun Zhou, Yiying Tong, and Kun Zhou. 2013. Face-warehouse: A 3d facial expression database for visual computing. *Transactions on Visualization and Computer Graphics* 20, 3 (2013), 413–425.
- [6] Feng-Ju Chang, Anh Tuan Tran, Tal Hassner, Iacopo Masi, Ram Nevatia, and Gérard Medioni. 2019. Deep, landmark-free FAME: Face alignment, modeling, and expression estimation. *International Journal of Computer Vision* 127, 6-7 (2019), 930–956.
- [7] Bindita Chaudhuri, Noranart Vesdapunt, and Baoyuan Wang. 2019. Joint face detection and facial motion retargeting for multiple faces. In Computer Vision and Pattern Recognition. 9719–9728.
- [8] Abhinav Dhall, Roland Goecke, Shreya Ghosh, Jyoti Joshi, Jesse Hoey, and Tom Gedeon. 2017. From individual to group-level emotion recognition: Emotiw 5.0. In ACM International Conference on Multimodal Interaction. 524–528.
- [9] E Friesen and Paul Ekman. 1978. Facial action coding system: a technique for the measurement of facial movement. *Palo Alto* 3 (1978).
- [10] Pablo Garrido, Michael Zollhöfer, Dan Casas, Levi Valgaerts, Kiran Varanasi, Patrick Pérez, and Christian Theobalt. 2016. Reconstruction of personalized 3D face rigs from monocular video. *Transactions on Graphics* 35, 3 (2016), 1–15.
- [11] Kyle Genova, Forrester Cole, Aaron Maschinot, Aaron Sarna, Daniel Vlasic, and William T Freeman. 2018. Unsupervised training for 3d morphable model regression. In Computer Vision and Pattern Recognition. 8377–8386.
- [12] Amogh Gudi, H Emrah Tasli, Tim M Den Uyl, and Andreas Maroulis. 2015. Deep learning based facs action unit occurrence and intensity estimation. In *Automatic Face and Gesture Recognition*, Vol. 6. IEEE, 1–5.
- [13] Philip Haeusser, Alexander Mordvintsev, and Daniel Cremers. 2017. Learning by Association—A Versatile Semi-Supervised Training Method for Neural Networks. In Computer Vision and Pattern Recognition. 89–98.
- [14] Kaiming He, Xiangyu Zhang, Shaoqing Ren, and Jian Sun. 2016. Deep residual learning for image recognition. In Computer Vision and Pattern Recognition. 770– 778
- [15] Jie Hu, Li Shen, and Gang Sun. 2018. Squeeze-and-excitation networks. In Computer Vision and Pattern Recognition. 7132–7141.
- [16] Sergey Ioffe and Christian Szegedy. 2015. Batch normalization: Accelerating deep network training by reducing internal covariate shift. arXiv preprint arXiv:1502.03167 (2015).
- [17] László A Jeni, Jeffrey M Girard, Jeffrey F Cohn, and Fernando De La Torre. 2013. Continuous au intensity estimation using localized, sparse facial feature space. In Automatic Face and Gesture Recognition. IEEE, 1–7.
- [18] Zi-Hang Jiang, Qianyi Wu, Keyu Chen, and Juyong Zhang. 2019. Disentangled representation learning for 3D face shape. In Computer Vision and Pattern Recognition. 11957–11966.
- [19] Sebastian Kaltwang, Ognjen Rudovic, and Maja Pantic. 2012. Continuous pain intensity estimation from facial expressions. In *International Symposium on Visual Computing*. Springer, 368–377.
- [20] Sebastian Kaltwang, Sinisa Todorovic, and Maja Pantic. 2015. Doubly sparse relevance vector machine for continuous facial behavior estimation. *Transactions on Pattern Analysis and Machine Intelligence* (2015), 1748–1761.
- [21] Sebastian Kaltwang, Sinisa Todorovic, and Maja Pantic. 2015. Latent trees for estimating intensity of facial action units. In Computer Vision and Pattern Recognition. 296–304.
- [22] Tero Karras, Samuli Laine, and Timo Aila. 2019. A Style-Based Generator Architecture for Generative Adversarial Networks. Computer Vision and Pattern Recognition (2019), 4401–4410.
- [23] Dieu Linh Tran, Robert Walecki, Stefanos Eleftheriadis, Bjorn Schuller, Maja Pantic, et al. 2017. Deepcoder: Semi-parametric variational autoencoders for automatic facial action coding. In *International Conference on Computer Vision*. 3190–3199.
- [24] Patrick Lucey, Jeffrey F Cohn, Takeo Kanade, Jason Saragih, Zara Ambadar, and Iain Matthews. 2010. The extended cohn-kanade dataset (ck+): A complete dataset for action unit and emotion-specified expression. In Computer Vision and Pattern Recognition-Workshops. IEEE, 94–101.
- [25] S Mohammad Mavadati and Mohammad H Mahoor. 2014. Temporal facial expression modeling for automated action unit intensity measurement. In *International Conference on Pattern Recognition*. IEEE, 4648–4653.

- [26] S Mohammad Mavadati, Mohammad H Mahoor, Kevin Bartlett, and Philip Trinh. 2012. Automatic detection of non-posed facial action units. In 2012 19th IEEE International Conference on Image Processing. IEEE, 1817–1820.
- [27] S Mohammad Mavadati, Mohammad H Mahoor, Kevin Bartlett, Philip Trinh, and Jeffrey F Cohn. 2013. Disfa: A spontaneous facial action intensity database. Transactions on Affective Computing 4, 2 (2013), 151–160.
- [28] Zuheng Ming, Aurélie Bugeau, Jean-Luc Rouas, and Takaaki Shochi. 2015. Facial action units intensity estimation by the fusion of features with multi-kernel support vector machine. In Automatic Face and Gesture Recognition, Vol. 6. IEEE, 1-6
- [29] Maja Pantic, Michel Valstar, Ron Rademaker, and Ludo Maat. 2005. Web-based database for facial expression analysis. In *International Conference on Multimedia* and Expo. IEEE, 5-pp.
- [30] P. Paysan, R. Knothe, B. Amberg, S. Romdhani, and T. Vetter. 2009. A 3D Face Model for Pose and Illumination Invariant Face Recognition. International Conference on Advanced Video and Signal based Surveillance for Security, Safety and Monitoring in Smart Environments.
- [31] Alec Radford, Luke Metz, and Soumith Chintala. 2015. Unsupervised representation learning with deep convolutional generative adversarial networks. arXiv preprint arXiv:1511.06434 (2015).
- [32] Elad Richardson, Matan Sela, and Ron Kimmel. 2016. 3D face reconstruction by learning from synthetic data. In *International Conference on 3D Vision*. IEEE, 460–469.
- [33] Ognjen Rudovic, Vladimir Pavlovic, and Maja Pantic. 2014. Context-sensitive dynamic ordinal regression for intensity estimation of facial action units. *Transactions on Pattern Analysis and Machine Intelligence* 37, 5 (2014), 944–958.
- [34] Georgia Sandbach, Stefanos Zafeiriou, and Maja Pantic. 2013. Markov random field structures for facial action unit intensity estimation. In *International Confer*ence on Computer Vision Workshops. 738–745.
- [35] Soubhik Sanyal, Timo Bolkart, Haiwen Feng, and Michael J Black. 2019. Learning to regress 3D face shape and expression from an image without 3D supervision. In Computer Vision and Pattern Recognition, 7763–7772.
- [36] Tianyang Shi, Yi Yuan, Changjie Fan, Zhengxia Zou, Zhenwei Shi, and Yong Liu. 2019. Face-to-Parameter Translation for Game Character Auto-Creation. In International Conference on Computer Vision. 161–170.
- [37] Patrick E Shrout and Joseph L Fleiss. 1979. Intraclass correlations: uses in assessing rater reliability. Psychological bulletin 86, 2 (1979), 420.
- [38] Karen Simonyan and Andrew Zisserman. 2014. Very deep convolutional networks for large-scale image recognition. arXiv preprint arXiv:1409.1556 (2014).
- [39] Xinhui Song, Tianyang Shi, Tianjia Shao, Yi Yuan, Zunlei Feng, and Changjie Fan. 2020. Unsupervised facial action unit intensity estimation via differentiable optimization. arXiv preprint arXiv:2004.05908 (2020).
- [40] Ayush Tewari, Michael Zollhöfer, Pablo Garrido, Florian Bernard, Hyeongwoo Kim, Patrick Pérez, and Christian Theobalt. 2018. Self-supervised multi-level face model learning for monocular reconstruction at over 250 hz. In Computer Vision and Pattern Recognition. 2549–2559.
- [41] Ayush Tewari, Michael Zollhofer, Hyeongwoo Kim, Pablo Garrido, Florian Bernard, Patrick Perez, and Christian Theobalt. 2017. Mofa: Model-based deep convolutional face autoencoder for unsupervised monocular reconstruction. In International Conference on Computer Vision Workshops. 1274–1283.
- [42] Anh Tuan Tran, Tal Hassner, Iacopo Masi, and Gérard Medioni. 2017. Regressing robust and discriminative 3D morphable models with a very deep neural network. In Computer Vision and Pattern Recognition. 5163–5172.
- [43] Dmitry Ulyanov, Andrea Vedaldi, and Victor Lempitsky. 2016. Instance normalization: The missing ingredient for fast stylization. arXiv preprint arXiv:1607.08022 (2016).
- [44] Michel Valstar and Maja Pantic. 2010. Induced disgust, happiness and surprise: an addition to the mmi facial expression database. In Proc. 3rd Intern. Workshop on EMOTION (satellite of LREC): Corpora for Research on Emotion and Affect. Paris, France., 65.
- [45] Michel F Valstar, Enrique Sánchez-Lozano, Jeffrey F Cohn, László A Jeni, Jeffrey M Girard, Zheng Zhang, Lijun Yin, and Maja Pantic. 2017. Fera 2017-addressing head pose in the third facial expression recognition and analysis challenge. In Automatic Face & Gesture Recognition. IEEE, 839–847.
- [46] Robert Walecki, Vladimir Pavlovic, Björn Schuller, Maja Pantic, et al. 2017. Deep structured learning for facial action unit intensity estimation. In Computer Vision and Pattern Recognition. 3405–3414.
- [47] Robert Walecki, Ognjen Rudovic, Vladimir Pavlovic, and Maja Pantic. 2016. Copula ordinal regression for joint estimation of facial action unit intensity. In Computer Vision and Pattern Recognition. 4902–4910.
- [48] Hao Wang, Yitong Wang, Zheng Zhou, Xing Ji, Dihong Gong, Jingchao Zhou, Zhifeng Li, and Wei Liu. 2018. Cosface: Large margin cosine loss for deep face recognition. In Computer Vision and Pattern Recognition. 5265–5274.
- [49] Xiang Wu, Ran He, Zhenan Sun, and Tieniu Tan. 2018. A light CNN for deep face representation with noisy labels. *Transactions on Information Forensics and Security* 13, 11 (2018), 2884–2896.
- [50] Hongwei Yi, Chen Li, Qiong Cao, Xiaoyong Shen, Sheng Li, Guoping Wang, and Yu-Wing Tai. 2019. Mmface: A multi-metric regression network for unconstrained

- face reconstruction. In Computer Vision and Pattern Recognition. 7663-7672.
- [51] Changqian Yu, Jingbo Wang, Chao Peng, Changxin Gao, Gang Yu, and Nong Sang. 2018. Bisenet: Bilateral segmentation network for real-time semantic segmentation. In European Conference on Computer Vision. 325–341.
- [52] Amir Zadeh, Tadas Baltrušaitis, and Louis-Philippe Morency. 2016. Deep constrained local models for facial landmark detection. arXiv preprint arXiv:1611.08657 3, 5 (2016), 6.
- [53] Xing Zhang, Lijun Yin, Jeffrey F Cohn, Shaun Canavan, Michael Reale, Andy Horowitz, Peng Liu, and Jeffrey M Girard. 2014. Bp4d-spontaneous: a highresolution spontaneous 3d dynamic facial expression database. *Image and Vision Computing* 32, 10 (2014), 692–706.
- [54] Yong Zhang, Weiming Dong, Bao-Gang Hu, and Qiang Ji. 2018. Weakly-supervised deep convolutional neural network learning for facial action unit intensity estimation. In Computer Vision and Pattern Recognition. 2314–2323.
- [55] Yong Zhang, Haiyong Jiang, Baoyuan Wu, Yanbo Fan, and Qiang Ji. 2019. Context-Aware Feature and Label Fusion for Facial Action Unit Intensity Estimation With Partially Labeled Data. In International Conference on Computer Vision. 733–742.
- [56] Yong Zhang, Baoyuan Wu, Weiming Dong, Zhifeng Li, Wei Liu, Bao-Gang Hu, and Qiang Ji. 2019. Joint representation and estimator learning for facial action unit intensity estimation. In Computer Vision and Pattern Recognition. 3457–3466.

- [57] Yong Zhang, Rui Zhao, Weiming Dong, Bao-Gang Hu, and Qiang Ji. 2018. Bilateral ordinal relevance multi-instance regression for facial action unit intensity estimation. In Computer Vision and Pattern Recognition. 7034–7043.
- [58] Zheng Zhang, Jeff M Girard, Yue Wu, Xing Zhang, Peng Liu, Umur Ciftci, Shaun Canavan, Michael Reale, Andy Horowitz, Huiyuan Yang, et al. 2016. Multimodal spontaneous emotion corpus for human behavior analysis. In Proceedings of the IEEE Conference on Computer Vision and Pattern Recognition. 3438–3446.
- [59] Zhanpeng Zhang, Ping Luo, Chen Change Loy, and Xiaoou Tang. 2014. Facial landmark detection by deep multi-task learning. In European Conference on Computer Vision. Springer, 94–108.
- [60] Rui Zhao, Quan Gan, Shangfei Wang, and Qiang Ji. 2016. Facial expression intensity estimation using ordinal information. In Computer Vision and Pattern Recognition. 3466–3474.
- [61] Xiangyu Zhu, Zhen Lei, Xiaoming Liu, Hailin Shi, and Stan Z Li. 2016. Face alignment across large poses: A 3d solution. In Computer Vision and Pattern Recognition. 146–155.
- [62] Xiangyu Zhu, Zhen Lei, Junjie Yan, Dong Yi, and Stan Z Li. 2015. High-fidelity pose and expression normalization for face recognition in the wild. In Computer Vision and Pattern Recognition. 787–796.